THE JOURNAL OF BIOLOGICAL CHEMISTRY VOL. 285, NO. 53, pp. 42001–42012, December 31, 2010

P0 (Protein Zero) Mutation S34C Underlies Instability of Internodal Myelin in S63C Mice*[S]

Received for publication, July 29, 2010, and in revised form, September 21, 2010 Published, JBC Papers in Press, October 11, 2010, DOI 10.1074/jbc.M110.166967

Robin L. Avila[‡1], Maurizio D'Antonio[§], Angela Bachi[§], Hideyo Inouye[‡2], M. Laura Feltri[§], Lawrence Wrabetz[§], and Daniel A. Kirschner[‡3]

From the [‡]Biology Department, Boston College, Chestnut Hill, Massachusetts 02467-3811 and the [§]Division of Genetics and Cell Biology, San Raffaele Scientific Institute, DIBIT 20132 Milan, Italy

P0 constitutes 50–60% of protein in peripheral nerve myelin and is essential for its structure and stability. Mutations within the P0 gene (*MPZ*) underlie a variety of hereditary neuropathies. *MpzS63C* transgenic mice encode a P0 with a serine to cysteine substitution at position 34 in the extracellular domain of mature P0 (P0S34C), associated with the hypomyelinating Déjérine-Sottas syndrome in human. S63C mice develop a dysmyelinating neuropathy, with packing defects in peripheral myelin. Here, we used x-ray diffraction to examine time-dependent packing defects in unfixed myelin. At ~7 h post-dissection, WT and S63C(+/+) myelin showed native periods (175 Å) with the latter developing at most a few percent swollen myelin, whereas up to ~50% of S63C(+/−) (mutant P0 on heterozygous P0 null background) or P0(+/−) myelin swelled to periods of ~205 Å. In the same time frame, S63C(−/−) myelin was stable, remaining swollen at ~210 Å. Surprisingly, treatment of whole S63C(−/−) nerves with a reducing agent completely reverted swollen arrays to native spacing and also normalized the swollen arrays that had formed in S63C(+/−) myelin, the genotype most closely related to the human disorder. Western blot revealed P0-positive bands at ~27 and ~50 kDa, and MALDI-TOF mass spectrometry showed these bands consisted of Ser^{34}-containing peptides or P0 dimers having oxidized Cys^{34} residues. We propose that P0S34C forms ectopic disulfide bonds in *trans* between apposed Cys^{34} side chains that retard wrapping during myelin formation causing hypomyelination. Moreover, the new bonds create a packing defect by stabilizing swollen membrane arrays that leads to demyelination.

P0, a single pass transmembrane protein, is the major structural protein of peripheral nerve myelin where it includes ~50% of the total protein (1). It has a characteristic immunoglobulin-like extracellular domain that is thought to underlie inter-membrane adhesion via homophilic interactions (2, 3). That P0 is the major structural adhesion molecule in PNS[4] myelin for membrane packing at both the cytoplasmic and extracellular appositions is based on structural analysis of myelin in the shiverer mouse, which lacks the myelin basic protein (MBP) in both CNS and PNS but yet has normal myelin arrays in the latter (4). Also consistent with this notion is the finding that P0 knock-out mice lack compaction of myelin (5). Observations on myelin in the shiverer/P0 double null mutant further support the role of P0 at the cytoplasmic apposition (6). One of the molecular contacts in crystals formed by the extracellular domain of P0 under physiological conditions is a 2-fold dimeric interaction between antiparallel molecules that is proposed to be at the adhesion interface between the apposed extracellular surfaces of myelin and to stabilize the native period and membrane packing (2).

Myelin protein zero (*MPZ*) mutations within the extracellular domain of P0 account for diverse peripheral neuropathies, including Charcot-Marie-Tooth, congenital hypomyelination, and early onset Déjérine-Sottas syndrome (DSS) (1, 7–9). Wrabetz *et al.* (10) produced and characterized a mouse model of DSS (7) in which a Ser → Cys substitution (P0S34C)[5] was introduced into the extracellular domain of P0. This mutation was proposed to produce disulfide aggregates (2, 11, 12) and a toxic gain of function in myelin (13). The mice develop neuromuscular dysfunction by 4–8 weeks of age, and their peripheral nerves show hypomyelination from early postnatal development and subsequent onion bulb formation, which may result from myelin degradation and failed attempts to remyelinate. Interestingly, nerves from the S63C transgenic mouse with varying amounts of endogenous P0wt (S63C(+/+) and S63C(+/−)) show by electron microscopy irregular areas of myelin swelling in a small subset of nerves. The disrupted areas correspond to the intraperiod line (where the extracellular domain is localized); therefore, the amino acid substitution may underlie the evident perturbation of the regular compaction of the membranes (10). By comparison, when P0S34C is expressed on a P0 null background (S63C(−/−)),

* This work was supported, in whole or in part, by National Institutes of Health Grants NS55256 and NS45630 from NINDS. This work was also supported by institutional funds from Boston College (to D. A. K.), Telethon, Italy, Grants GGP07100 and GGP08021, and European Community Grants NGIDD-HEALTH-F2-2008-201535 (to L. W. and M. L. F.).

[S] The on-line version of this article (available at http://www.jbc.org) contains supplemental Table 1, Figs. 1–4, and datasets.

[1] Present address: Dept. of Neurology, University of Chicago, 5835 S. Cottage Grove Ave., Chicago, IL 60637.

[2] Present address: X-ray Analysis Division, Rigaku Corp., 3-9-12, Matsubaracho Akishima-shi, Tokyo 196-8666, Japan.

[3] To whom correspondence should be addressed: Biology Dept., Boston College, 140 Commonwealth Ave., Chestnut Hill, MA 02467-3811. Tel.: 617-552-0211; Fax: 617-552-2011; E-mail: kirschnd@bc.edu.

[4] The abbreviations used are: PNS, peripheral nervous system; MBP, myelin basic protein; TCEP, Tris(2-carboxyethyl)phosphine hydrochloride; NEM, *N*-ethylmaleimide; DSS, Déjérine-Sottas syndrome; IAA, iodoacetamide; NF, neurofilament; XRD, x-ray diffraction.

[5] In this paper we number the residues according to the processed protein. For the preprotein, which includes the signal peptide, the mutation is referred to as S63C.

electron microscopy reveals uniform areas of myelin swelling apparently due to widening of the extracellular apposition by 21% (10).

To explore in detail the inferred instability of myelin in S63C transgenic mouse lines, we analyzed myelin structure in whole, unfixed sciatic nerves using x-ray diffraction (XRD). This technique provides a sensitive and quantitative assessment of internodal myelin structure, membrane packing, and interactions in both a native environment or after physical/chemical treatment (14). As the measurements are carried out on a large volume of nerve rather than just thin sections, there is abundant sampling of internodal myelin (15). In preliminary experiments, we found that the myelin period in nerves from S63C(+/−) resembles that of the native state (175 Å), but after ~7 h a significant amount of myelin swells to 205-Å period arrays (10). Furthermore, myelin from S63C(−/−) shows an ~210-Å period, which is significantly larger than the ~190-Å period for P0(−/−). These initial results suggest that the myelin packing depends on the amount of P0wt and that above a certain ratio of mutant *versus* WT protein, the former causes instability or dominates the dimeric adhesion interface because of aberrant interactions. Our objective here was to explore further the varied phenotypes of the P0S34C mutation by using XRD to quantitate the packing defects in freshly dissected nerves and in nerves subjected to electrostatic stress (different pH and ionic strength). We found the following: 1) the instability of P0(+/−) myelin derives from the lower level of P0wt, which provides fewer homophilic contacts at the dimeric adhesion interface; 2) the instability of S63C(+/−) myelin derives from the presence of mutant protein, as the total amount of P0 mRNA is nearly twice the wild type level; 3) the presence of the mutant protein renders the myelin more sensitive to pH changes, because of altered interactions involving His^{52} and $Arg^{45'}$ near the dimeric adhesion interface; 4) in the absence of any P0wt, formation of a new disulfide between Cys^{34} and $Cys^{34'}$ stabilizes swollen myelin arrays; and 5) swollen myelin containing the mutant protein can be "cured" by subjecting the nerve to a reducing agent.

EXPERIMENTAL PROCEDURES

Transgenic Mice

The mice used to analyze myelin structure were bred and maintained on the FVB/N inbred strain at the San Raffaele Scientific Institute (Milano, Italy) and included the following: wild type (WT; P0(+/+)), P0 heterozygous (P0(+/−)), P0null ($P0^{null}$ or P0(−/−)), and S63C on the WT, heterozygous, and null backgrounds (S63C(+/+), S63C(+/−), and S63C(−/−)). The S63C mice have a serine to cysteine substitution at position 34 in the extracellular domain of the processed protein (10). These mice correspond to the line Tg130.3, Tg(MpzS63C)33Mes. Tg130.3 and heterozygous-null mice were crossed to generate the P0S34C mutation on backgrounds with different expression levels of P0wt, resulting in S63C(+/+) (2.2-fold overexpression of P0wt and P0S34C mRNA), S63C(+/−) (1.7-fold overexpression of total P0 mRNA both P0wt and P0S34C mRNAs), and S63C(−/−) (1.2-fold overexpression of P0S34C mRNA).

X-ray Diffraction

Sample Preparation—Sciatic nerves were dissected from wild type and transgenic mice that had been sacrificed by cervical dislocation and decapitation. During dissection, the tissue was continually rinsed with physiological saline (154 mM NaCl, 5 mM Tris base, pH 7.4). After being tied off at each end with fine suture, the nerves were pulled into 0.7–0.9-mm capillary tubes (Charles Supper Co., South Natick, MA) containing the appropriate solution, and the tubes were sealed at both ends with wax. For electrostatic stressing (16), the sciatic nerves were stretched slightly onto a frame (a notched, plastic pipette tip) and placed into scintillation vials containing 20-ml aliquots of solutions of known ionic strength and pH (see below), gently agitated overnight, and then loaded into quartz capillary tubes as described above.

Solutions used were as follows: normal physiological saline, either 154 mM NaCl, 5 mM Trizma® base (tris[hydroxymethyl]-aminomethane) titrated with HCl to pH 7.4, or 154 mM NaCl, 5 mM phosphate buffer, adjusted to each desired pH 6–8; hypotonic alkaline saline, 60 mM NaCl and 30 mM NaCl, 5 mM Trizma® base titrated with NaOH to pH 8, and 30 mM NaCl, 5 mM glycine titrated with NaOH to pH 9; hypotonic acidic saline, 60 mM NaCl, 5 mM glycine titrated with HCl to pH 3.1 or 2.1, and 30 mM NaCl, 5 mM glycine buffer titrated with HCl to pH 2.1; alkaline saline, 154 mM NaCl, 5 mM glycine buffer titrated with NaOH to pH 10–10.5. The reducing solution consisted of 10 or 50 mM Tris(2-carboxyethyl)phosphine hydrochloride (TCEP; catalog no. 20490, Pierce) (17, 18), 154 mM NaCl, and 5 mM Trizma® base, titrated with NaOH to pH 7.4.

For preliminary screening of myelin structure, we examined nerves fixed by immersion in 2% glutaraldehyde in 0.12 M phosphate buffer at pH 7.4, maintained in the same fixative during shipment from the San Raffaele Institute (Milano, Italy) to Boston College, and kept in fixative during x-ray diffraction. These findings, which revealed hypomyelination, specifically a one-third decrease in the relative amount of myelin for S63C(+/+) *versus* WT (supplemental Fig. 1), encouraged us to proceed with analysis of unfixed myelin from whole nerves, as described here.

Perfusion Chamber—To better preserve physiological conditions for nerve, we used a perfusion chamber that allowed continuous flow of solution over the nerve during 20 h of intermittent x-ray data collection. A peristaltic pump (Masterflex, Cole-Parmer, Vernon Hills, IL) maintained the flow from a 300-ml reservoir.

X-ray Diffraction and Myelin Structure Analysis—The experimental details have been described in recent publications (10, 15, 19, 20). Briefly, x-ray diffraction patterns from whole sciatic nerves, freshly dissected from the mice or after overnight treatment under defined conditions, were recorded using an electronic detector. The myelin period (d) was directly measured from the positions of the intensity maxima. After background subtraction, the area of the peaks (or integrated intensities) were used to calculate structure amplitudes that were used to calculate the membrane profiles via Fourier synthesis. From the profiles we measured the inter-membrane spaces at the cytoplasmic and extracellular appositions, and

the thickness of the lipid bilayer. Such a calculation was undertaken for diffraction data to ~30 Å spacing (14). Whereas for native sciatic nerve myelin, a sufficient number of reflections were present, for swollen myelin this occurred only when the swollen phase was the predominant one and had multiple Bragg orders, *e.g.* S63C(−/−) and P0(−/−). The relative amount of internodal myelin was expressed as $M/(M+B)$, where M is the total integrated intensity of the myelin reflections after background (B) subtraction, and $M+B$ is the total intensity. A scatterplot of $M/(M+B)$ *versus* myelin period was used to compare the different genotypes (supplemental Figs. 1 and 2). The irregularity (or distortion) in membrane packing (denoted by lattice parameter Δ) was determined by analyzing the peak widths of reflections (15, 21, 22) and was expressed here as a fraction of the periodicity d, or Δ/d. The significance of the difference between the means for different parameters was evaluated using the Student's t test, with $p < 0.05$ considered significant.

Western Blotting

Myelin was isolated from sciatic nerves of adult mice, as described previously (Ref. 23 with modifications), separated by SDS-PAGE (Fig. 5, *A* and *B*) using a pre-cast 4–20% Tris-glycine gradient gel (1.0 mm, 12 wells; Invitrogen), and analyzed by Western blot as described (Fig. 5*C* and supplemental Fig. 3) (10). For SDS-PAGE, the sample buffer, pH 6.8, contained 2% SDS, 63 mM Tris base, 10% glycerol, and 0.01% bromphenol blue. Isolated myelin samples were loaded and run in an XCELL Surelock™ mini-cell (Invitrogen) for 1–2 h at a constant 125 V. For Western blotting, proteins were electrophoretically transferred onto an Immobilon-P PVDF transfer membrane (Bio-Rad) using an XCell II™ blot module (Invitrogen). Proteins were detected using the ECL™ Western blotting detection reagents and analysis system (GE Healthcare). The membrane was incubated for 1 h with either a 1:2000 dilution of a rabbit polyclonal anti-P0 primary antibody (kindly provided by Dr. David Colman via Dr. Brian Popko), a 1:2000 dilution of a mouse monoclonal anti-P0 primary antibody (P07, kindly provided by Dr. Juan Archelos), or a 1:1000 dilution of polyclonal anti-MBP primary antibody (Santa Cruz Biomedical, Santa Cruz, CA). Proteins were visualized by chemiluminescence according to the manufacturer's instructions, using a peroxidase-labeled anti-rabbit or anti-mouse secondary antibody at 1:10,000 dilution and ECL™ detection reagents. Molecular mass markers were MagicMark (Invitrogen).

Protein Identification by Matrix-assisted Laser Desorption/Ionization-Time of Flight-Mass Spectrometry (MALDI-TOF MS) Analysis

Myelin was isolated from mouse sciatic nerves (as described above) with the addition of 10 mM *N*-ethylmaleimide (NEM) to the reagents, so all the cysteines present as free thiols in myelin would be NEM-alkylated (supplemental Fig. 4). After SDS-PAGE, the bands of interest were excised from the gel, subjected to reduction by 10 mM DTT and alkylation by 55 mM iodoacetamide (IAA), and finally digested with trypsin overnight (Roche Applied Science) (24). 1-μl aliquots of the supernatant were used for MS analysis on a MALDI-TOF Voyager-DE STR (Applied Biosystems) mass spectrometer using the dried droplet technique and α-cyano-4-hydroxycinnamic acid as matrix. In parallel, bands already treated with trypsin were further digested with Asp-N enzyme overnight (Roche Applied Science); the supernatants were used for MALDI-TOF MS analysis. Peak list was obtained by peak deisotoping. Spectra were accumulated over a mass range of 750–4000 Da with a mean resolution of about 15,000. Spectra were internally calibrated using matrix signals and trypsin autolysis peaks and then processed via Data Explorer software version 4.0.0.0 (Applied Biosystems). Searches were performed with trypsin and Asp-N specificity; cysteine alkylation by IAA, NEM, and oxidation of methionine were considered as variable modifications. Two missed cleavages per peptide were allowed, and an initial mass tolerance of 50 ppm was used in all searches. Peptides with masses corresponding to those of enzymes and matrix were excluded from the peak list. Proteins were identified by searching a comprehensive nonredundant protein data base (NCBInr 20080912 (7031513 sequences; 2427977331 residues) Taxonomy:Rodentia (222606 sequences)) using Mascot (Matrix Science; version 2.1.04) program.

RESULTS

Chemical stabilization of myelin by aldehyde fixation results in changes in periodicity and membrane packing (25); however, such tissue is useful for an initial screening of myelinated nerves that may have altered amounts of internodal myelin (15). Preliminary screening of glutaraldehyde-fixed sciatic nerves from S63C(+/+) mice revealed consistently weaker myelin diffraction patterns compared with WT nerves. Quantitation showed that there was about one-third less internodal myelin in the transgenic nerves but that the myelin periodicities were not significantly different between the genotypes (supplemental Fig. 1). A preliminary XRD study of the unfixed nerves from S63C mice and electron microscopy of embedded tissue substantiated the hypomyelination (10) and provided the rationale for the current, more systematic study of myelin structural integrity in the S63C genotype series.

Myelin-containing Mutant P0S34C Swelled in Sealed Capillary—Diffraction patterns were recorded from the freshly dissected sciatic nerves of mice with genotypes WT, S63C(+/+), S63C(+/−), S63C(−/−), and P0(+/−). Recorded within 30 min of dissection, the initial 10-min patterns of the nerves, which had been sealed into capillaries containing excess physiological saline, revealed obvious differences in the relative intensities of the patterns and in myelin periods (Fig. 1*A*; Table 1). From strongest to weakest, the patterns ranked as follows: WT > P0(+/−) > S63C(+/+) ≈ S63C(+/−) > S63C(−/−) > P0(−/−) (null not shown; see Ref. 15). Native periods (~175 Å) were observed for WT and for S63C on the WT and heterozygous backgrounds, and larger periods were recorded for P0(+/−) (~5 Å greater than native), P0(−/−) (~10 Å greater), and S63C on the null background (>30 Å greater). Close inspection of the pattern from S63C(+/−) showed elevated intensity between the 2nd and

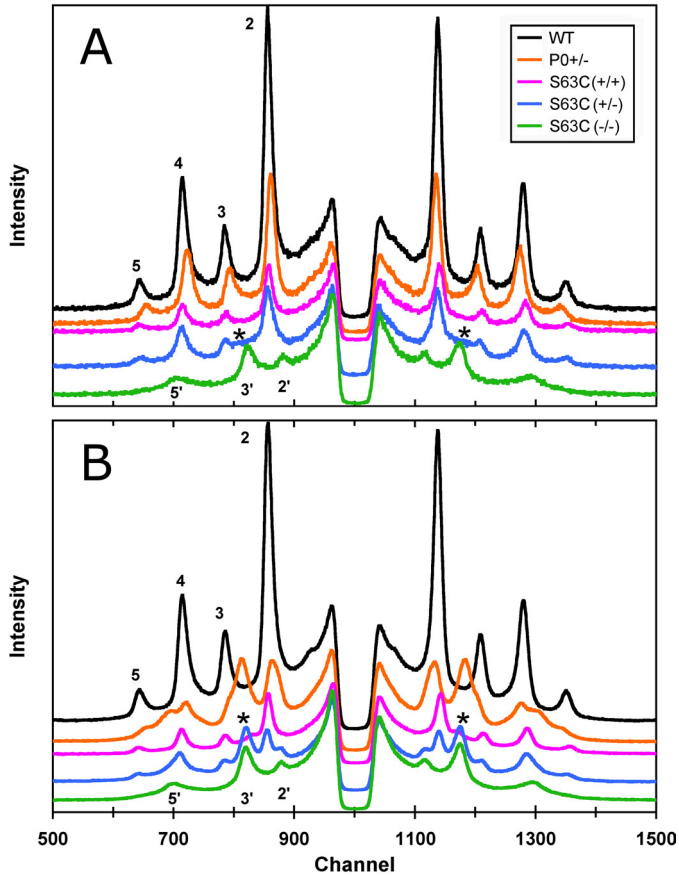

FIGURE 1. **X-ray patterns from unfixed sciatic nerve of WT, S63C(+/+), S63C(+/−), S63C(−/−), and P0(+/−) transgenic mice.** *A,* nerves were sealed in capillaries containing physiological saline. Initial 10-min exposure patterns were recorded immediately after dissection. The patterns have been shifted on the *y* axis for clarity. Bragg orders 2–5 from the native WT, 175-Å period myelin, and 2′, 3′, and 5′ from the ~210- and 205-Å period swollen arrays of S63C(−/−) and S63C(+/−) are indicated. The *asterisk* in the latter indicates high background where diffraction from another phase is beginning to form. *B,* each 2-h exposure was begun 7 h after dissection. Native 175 Å arrays remained only for WT; all the others were either completely swollen (S63C(−/−)) or show two arrays (S63C(+/−), P0(+/−), and S63C(+/+)). The *asterisks* in S63C(+/+) denote a peak beginning to form, similar to what was seen initially in S63C(+/−).

3rd Bragg reflections (Fig. 1*A*, *asterisk*), which corresponded in position to the predominant intensity maximum from the swollen myelin of S63C(−/−) (Fig. 1, *peak labeled 3′*). To check for stability of the myelin period and membrane packing, we recorded a subsequent pattern from each nerve about 7 h after the initial pattern (Fig. 1*B*). Four of the nerves gave patterns virtually identical to the originals as follows: the WT (175 Å) and S63C on the WT background, P0(−/−) (187 Å), and S63C on the null background (207 Å). By contrast, P0(+/−) and S63C(+/−) both showed complex patterns indicating new ~200-Å period swollen arrays coexisting with native arrays. Measurement of the intensities indicated that there were approximately equal amounts of each type of array. Although its predominant structure was native, the myelin with S63C(+/+) showed an increase in background intensity between the 2nd and 3rd Bragg reflections (*, Fig. 1*B*) indicating a small amount of swollen myelin. Calculation of membrane profiles (data not shown) from the diffraction data revealed that the larger period was accounted for by ~30 Å swelling at the extracellular apposition in S63C(−/−) and ~10 Å swelling in P0(−/−) (Table 1).

S63C(+/−) and P0(+/−) Also Swelled under More Physiological Conditions—As rat spinal roots (PNS) incubated in a sealed capillary tube undergo swelling over time, probably due to anoxic conditions within the microenvironment (26), we determined whether anoxia was a factor in the swelling of the mutant nerve myelin. Nerves were bathed continuously for ~20 h from a large reservoir of physiological saline that was exposed to the air, and x-ray patterns were periodically recorded. Myelin in WT and S63C(+/+) nerves was stable throughout the 20 h and exhibited the same native periodicity (Fig. 2, *A* and *B*; Table 2). S63C(+/−) initially had a native period (Fig. 2*C*), but by 5 h, the sciatic nerve had developed an increase in background scatter between the 2nd and 3rd Bragg order reflections (Fig. 2*C*, *; Table 2), which by 20 h corresponded to be the 3rd order of an ~221-Å period array. Quantitation of the diffracted intensity indicated that this swollen array accounted for about one-tenth of the ordered myelin. P0(+/−) exhibited a consistent 180-Å period for ~5 h of perfusion (Fig. 3*E*), and by 20 h had developed distinct 205-Å period swollen arrays (Bragg orders denoted by 2′, 3′, and 5′). The swollen arrays accounted for one-fifth of the total intensity of the ordered myelin (Table 2). Both S63C(−/−) and P0(−/−) maintained stable swollen arrays during the perfusion, with the periodicity for the myelin containing the mutant protein remaining about 15 Å greater than that for the null mutant (Fig. 2, *D* and *F*; Table 2).

pH-induced Swelling for S63C(+/−) and P0(+/−) Myelin Differed from WT—Inter-membrane stability at the extracellular apposition of myelin is thought to depend on the homophilic interactions between apposed P0 molecules, which involves the His^{52} and $Arg^{45'}$ residues at the 2-fold dimeric adhesion interface (2). As this polar interaction is likely to be labile to changes in pH (16) and also to be affected by the substitution of the proximal residue Ser^{34} by Cys, we investigated whether the panel of S63C genotypes was differentially affected by changes in pH.

Sciatic nerves were treated with solutions ranging from pH 6 to 8 (Fig. 3, *A* and *B*; supplemental Table 1). Previously, it had been shown for WT mouse sciatic myelin that decreasing the pH to 6.5–7.0 causes swelling (16). The resulting threshold for such swelling was at a higher pH ~7.5 for both S63C(+/−) and P0(+/−) as follows: S63C(+/−) had two phases (174 and 232 Å), the latter accounting for a few percent of ordered myelin; and P0(+/−) had two phases (180 Å and 217 Å), where the swollen arrays constituted 13% of the myelin (supplemental Table 1). Compaction to the native period for these nerves occurred in the range pH 7.6–8, indicating that they are more stable at alkaline pH. The threshold for S63C(+/+) was closer to that of WT, as at pH 7.0 only a small amount of swelling (~3%) was evident. By contrast with these genotypes, S63C(−/−) myelin throughout the entire pH range displayed a swollen period of ~209 ± 4 Å, suggesting that some specific interaction may underlie stability of the swollen period. The period for P0(−/−) in the same pH range was 191 ± 7 Å. Thus, the presence of the mutant P0 in the absence of P0wt resulted in a stable membrane separation

TABLE 1

Stability of sciatic nerve myelin in a sealed capillary

− indicates dimensions absent because of insufficient resolution of the x-ray pattern (see "Experimental Procedures").

Time[a]	Dimensions[b]				Δ/*d*[c]	Myelin[d]	*M*/(*M*+*B*)[e]
	d	cyt	lpg	ext			
	Å					%	
WT							
10 min	175.0	31	48	48	0.023		0.35
7 h	174.8	31	49	46	0.017		0.35
S63C(+/+)							
10 min	174.3	31	47	49	0.029		0.17
7 h	173.1	32	46	49	0.029	95	0.15
	~219	−	−	−		5	
S63C(+/−)							
10 min	174.9	31	48	49	0.029	92	0.21
	~210	−	−	−		8	
7 h	173.2	−	−	−	0.023	59	0.21
	204.7	−	−	−		41	
S63C(−/−)							
10 min	210.7	33	49	80	0.057		0.13
7 h	207.0	31	50	76	0.048		0.11
P0(+/−)							
10 min	180.1	30	50	50	0.028		0.28
7 h	180.2	31	49	51	0.022	45	0.36
	197.7	−	−	−		55	
P0(−/−)							
10 min	187.3	−	−	−	0.048		0.06
7 h	187.0	33	46	62	0.043		0.04

[a] Myelin structure was assessed by XRD immediately after dissection and 7 h later.

[b] The abbreviations used are as follows: *d,* myelin period, as measured from the diffraction spectra; cyt, cytoplasmic apposition; lpg, separation between lipid polar head group layers; ext, extracellular apposition; all as determined from the membrane density profiles (see "Experimental Procedures" for details).

[c] The irregularity in the packing of myelin membranes was determined from the breadths of the x-ray reflections (15) and expressed as a fraction of the periodicity *d*.

[d] The percentage of the total myelin that is in the swollen state, calculated from $P_i = \Sigma_h (hI_i(h)/d_i^2)$ (50), where $I(h)$ is the integrated intensity of the peak corresponding to the hth Bragg order, and d is periodicity.

[e] Relative amount of compact myelin $M/(M+B)$ (see "Experimental Procedures").

that in swollen myelin was nearly 20 Å greater than without the protein. Moreover, in the linear regressions for these data, the standard error for the periodicity in S63C(−/−) myelin was nearly one-third that for the P0(−/−) myelin, suggesting an intermembrane stabilizing interaction in the former.

Comparison of Membrane Packing Regularity among the Genotypes—To analyze the disorder in the stacking of the myelin membranes, we plotted the integral widths of the x-ray reflections w^2 *versus* the Bragg order h^4 for the different sets of diffraction data from the six genotypes examined in this study (see "Experimental Procedures") (15). The membrane packing disorder (Δ/*d*) in S63C(−/−) was nearly double that in the wild type and heterozygous (S63C(+/−)) myelins; and the mutation resulted in less regular packing of lamellae than membranes totally lacking P0 (Table 1). Overall, when ranked from greatest to least packing regularity (expressed as Δ/*d*), the genotypes were as follows: WT > S63C(+/+) ≈ S63C(+/−) ≈ P0(+/−) > P0(−/−) > S63C(−/−). (The significance levels for this comparison ranged from $p < 0.0001–0.04$.)

Reducing Agent Reverted Swollen Myelin of S63C(+/−) to Native Spacing—That the extracellular domains of P0 interact homophilically and the substituted residue is located toward the apex of this domain raised the possibility that formation of a new disulfide between Cys^{34} and $Cys^{34'}$ (2, 11, 13) could account for the stability of the swollen membranes in S63C(−/−). To test this idea, we used TCEP as a reducing agent in which to incubate the S63C nerves. TCEP is a thiol-free reducing agent that is proposed to be more effective than either dithiothreitol (DTT) or mercaptoethanol, and it has the advantages of stoichiometric reduction (1 mol of TCEP reduces 1 mol of protein disulfide), no detection in modifications of other residues other than cysteine, and being nonvolatile, water-soluble, and odorless (17).

Experiments in parallel were undertaken with WT nerves to control for the possibility that TCEP might also reduce the disulfide that stabilizes the β-sheets within the extracellular domain (2). Membrane packing effects were assessed by analysis of the diffraction patterns after 15–20 h of incubation of nerves in 0, 10, and 50 mM TCEP (added to physiological saline at pH 7.4). WT myelin retained a native or near-native period (Fig. 4*A*; Table 3), whereas the swollen myelin of both S63C(+/−) and S63C(−/−) reverted to the native period with TCEP treatment (Fig. 4, *B* and *C*; Table 3). At 10 mM TCEP, both swollen and native period arrays were detected in the S63C(−/−) nerve. The membrane profiles calculated from the diffraction data showed an ~36-Å decrease in width of the extracellular apposition (Table 3). When S63C(−/−) compacted to the native period, the myelin became more regularly packed (Table 3; Δ/*d*).

Western Blotting and MALDI-TOF MS Confirmed Novel Disulfide Formation—To demonstrate chemically whether P0S34C forms intermolecular disulfide bonds in myelin, we performed SDS-PAGE on purified myelin from WT, S63C(+/+), S63C(+/−), and S63C(−/−) adult nerves, under reducing or nonreducing conditions (Fig. 5). Using either a rabbit polyclonal (Fig. 5*A*) or a mouse monoclonal (Fig. 5*C*) anti-P0 antibody, we could clearly detect in all samples under nonreducing conditions a band of relative mobility of ~27

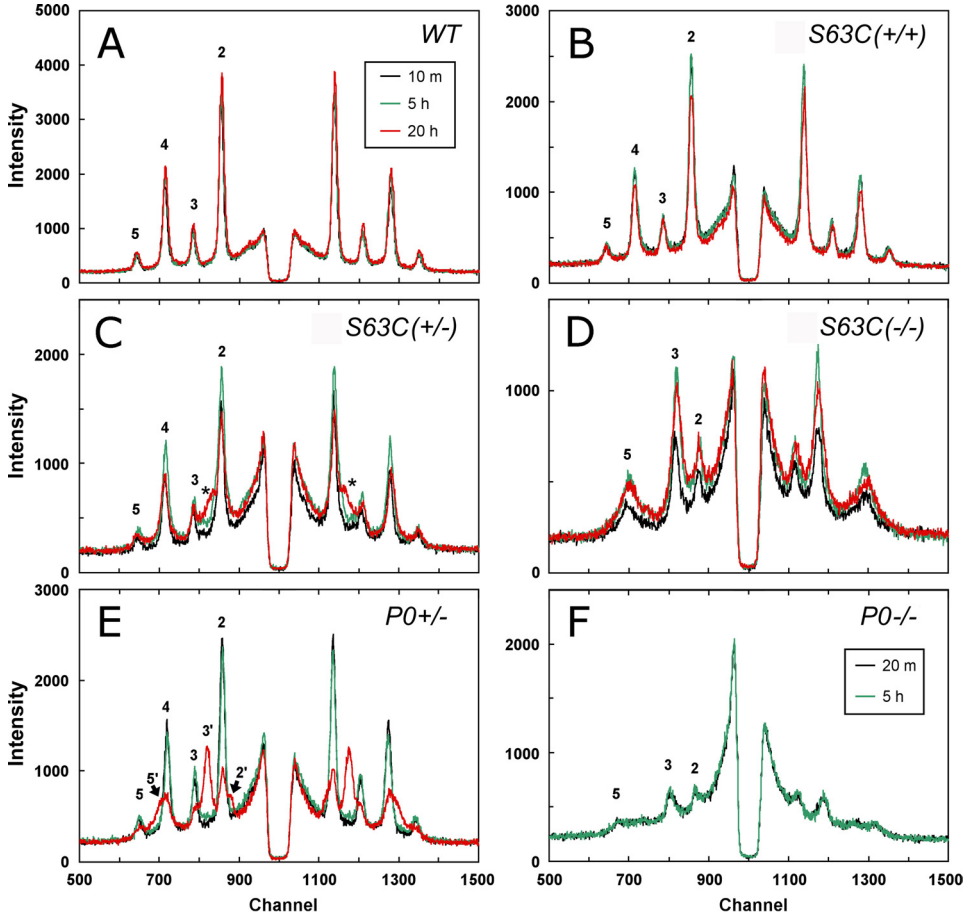

FIGURE 2. **X-ray patterns for the various genotypes during perfusion of the nerves with physiological saline, recorded immediately after dissection, and after 5 and 20 h.** *A*, WT; *B*, S63C(+/+); *C*, S63C(+/−); *D*, S63C(−/−); *E*, P0(+/−); and *F*, P0(−/−). Each spectrum is the data collected for a duration of 10 min, and Bragg orders 2–5 are indicated if visible. *A*, WT showed a stable period of 175 Å throughout the 20-h perfusion. *B*, S63C(+/+) showed a stable period similar to that of the WT. *C*, S63C(+/−) showed the formation of a new reflection (*) as the perfusion time increased. *D*, S63C(−/−) showed a constant swollen period of ~207 Å for the entire duration. *E*, P0(+/−) showed a stable period of 178 Å for at least 5 h but then developed a swollen phase. *F*, P0(−/−) showed a constant period of 191 Å, which was smaller than that observed for S63C(−/−) (207 Å).

kDa (the expected size of WT P0, *) and in the S63C(−/−), S63C(+/−), S63C(+/+) samples, a band at ~50 kDa (*arrowhead*) that disappeared after treatment with reducing agents. Neither of these bands was detected in sciatic nerve extracts from P0(−/−) mice after blotting with the same antibodies (supplemental Fig. 1 and data not shown), indicating that these two bands represented P0.

To characterize the proteins present in the 27- and 50-kDa bands, myelin was purified with NEM-containing reagents to alkylate all cysteines present as free thiols and then subjected to SDS-PAGE. The bands of interest were then excised from the gel (Fig. 5*C*) and subjected to MALDI-TOF MS. The ~27-kDa band consisted of peptides containing either Ser^{34} or Cys^{34}, whereas the ~50-kDa band consisted only of peptides containing Cys^{34} (supplemental Fig. 4 with supplemental datasets). Importantly, in the 50-kDa band, the peptides containing Cys^{34} were all found modified with IAA, indicating that the Cys had been in the oxidized form in myelin and that it had been reduced only after extraction from the gel (Fig. 5*D* and supplemental Fig. 4). By contrast, peptides containing Cys^{34} in the 27-kDa band were found modified with both NEM (meaning that they were as free thiol in the cell lysate) and IAA (Fig. 5*D* and supplemental Fig. 4). This analysis provides further evidence supporting the hypothesis that Cys^{34} is involved in abnormally positioned disulfide bond formation in myelin.

DISCUSSION

Initial Screening of Sciatic Nerve Myelin from S63C Mice—Aldehyde fixation of WT nerves introduces small alterations in myelin packing (25), which are mostly in periodicity and membrane structure rather than in relative amount of myelin (15). For this study, an initial assessment of fixed sciatic nerve by XRD showed that the S63C(+/+) had about one-third less internodal (compact) myelin than WT (supplemental Fig. 1). Subsequently, XRD results from a limited sample of unfixed S63C nerves suggested reduced amounts of myelin, altered periodicity, and instability; and EM analysis of S63C(+/+) myelin revealed irregular areas of expansion in small subsets of the myelin lamella (10). As a result of these findings, we conducted a systematic study of freshly dissected nerves from the various genotypes of S63C transgenic mice to determine in unfixed nerves (native conditions) the amount and localization of packing disorder and myelin instability.

Instability of S63C Myelin—Initial diffraction patterns of S63C(+/−) revealed that there are two myelin periods at

TABLE 2

Stability of sciatic nerve myelin during perfusion

Myelin structure in nerves mounted in a perfusion chamber was assessed by XRD; patterns were recorded immediately after dissection and at 5 and 20 h during the perfusion with physiological saline. See legend to Table 1 for details.

Time	Dimensions				Δ/*d*	Myelin	*M*/(*M*+*B*)
	d	cyt	lpg	ext			
	Å					%	
WT							
10 min	174.7	31	48	47	0.023		0.38
5 h	174.7	31	48	47	0.023		0.42
20 h	174.7	31	48	47	0.023		0.41
S63C(+/+)							
10 min	175.3	31	49	46	0.023		0.30
5 h	175.1	31	49	46	0.023		0.31
20 h	174.4	30	49	46	0.023		0.29
S63C(+/−)							
10 min	175.9	33	47	49	0.028		0.23
5 h	175.9	33	47	49	0.023	95	0.27
	196.5					5	
20 h	174.7	31	47	49	0.029	88	0.25
	220.5					12	
S63C(−/−)							
10 min	206.0				0.049		0.14
5 h	208.4				0.048		0.15
20 h	205.4				0.054		0.21
P0(+/−)							
10 min	179.5	33	48	50	0.028		0.29
5 h	180.6	33	50	48	0.028		0.27
20 h	181.9	34	49	50	0.033	79	0.21
	204.6					21	
P0(−/−)[a]							
20 min	191.2				0.037		0.10
5 h	191.7				0.042		0.09

[a] P0(−/−) sciatic nerve was too weak to withstand lengthy perfusion, so only data at 5 h are shown.

physiological pH (pH 7.4), 175 and ~210 Å (Fig. 1; Table 2). S63C(+/+) and P0(+/−) myelin swelled after 7 h in the sealed capillary tube, whereas S63C(−/−) maintained a stable ~210-Å period. The relative amount of myelin for S63C(+/+), S63C(+/−), and S63C(−/−) was reduced by about one-half, consistent with the idea that the S34C mutation causes hypomyelination along with demyelination, as indicated by EM (10). When the S63C(+/−) sciatic nerves were examined after 7 h in a sealed capillary tube, the percentage of swollen myelin increased, suggesting myelin instability. Previous studies have shown that treatment of PNS nerves under anoxic conditions, *e.g.* in an oxygen-deprived environment such as a sealed capillary, may cause myelin swelling (26). Metabolism of cellular glucose without oxygen might decrease the pH, causing the myelin to swell (16). To test whether anoxia caused the swelling, nerves were placed in a perfusion chamber that allowed for the continuous flow of aerated physiological saline over the nerve during recording of the XRD patterns (Fig. 2; Table 2).

Diffraction from perfused S63C sciatic nerve demonstrated that over a duration of 20 h the S63C(+/−) myelin still swelled (to ~210 Å), and the swelling started as early as 5 h and progressed to account for about 12% of the myelin (Table 2). This result suggests that the instability of myelin in the transgenic sciatic nerves was due to the mutation itself and not to anoxia. P0(+/−) sciatic nerve also showed instability, as it developed a swollen phase after 20 h of perfusion. The instability of P0(+/−) is most likely due to fewer homophilic contacts because of the lowered amount of WT P0. Perfusion of S63C(−/−) for 20 h revealed that the swollen myelin membranes were stable, even though the myelin was less ordered (Fig. 2*D*; Table 2).

S63C(+/−) Nerve Displayed Myelin Stability at More Alkaline pH—The effects of pH and ionic strength on membrane-membrane interactions in myelin have been determined by XRD measurements on nerves from normal (16) and transgenic (10, 15, 20, 27) mice. These studies demonstrate that at physiological ionic strength WT nerves transition from a compact phase (~165 Å) at pH 4–5 to a swollen phase (~220 Å) at pH 5–7 and to a native phase (~176 Å) at pH 7–10. Here, we treated nerves at different pH values to detect membrane packing alterations arising from the Cys^{34} mutation. S63C(+/−) did not transition to a native phase until at pH >7.6, unlike WT that transitioned at pH 6.6 (Fig. 3; supplemental Table 1). This result indicates that myelin membrane interactions in S63C(+/−) at physiological ionic strength depends on pH for stability. By contrast, S63C(−/−) did not switch at all to the native period structure, indicating that the Cys^{34} mutation somehow contributes to stabilizing the swollen array. The myelin containing only one copy of the Mpz^{wt} (P0(+/−)) also showed a swollen period until more alkaline pH, apparently due to a P0 dosage effect.

Studies on the amino acid substitution Ser →Cys in the P0 extracellular domain show that the mutant P0S34C is incorporated into the sheath, where it produces packing defects (10). The sciatic nerves of S63C mice exhibit onion bulb formation and have thinner sheaths, which are compatible with the DSS phenotype in humans (28). Because of P0 dosage, a valid model of S34C could not be produced with one mutant allele and one WT allele, due to the resultant overexpression

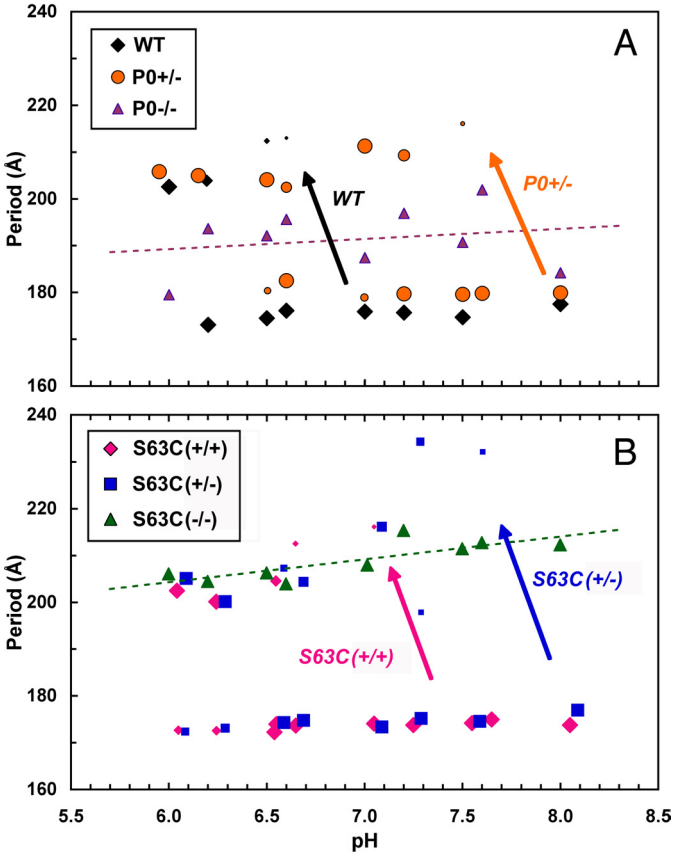

FIGURE 3. **Differential stability of sciatic nerve myelin for the various genotypes, depicted as myelin period *versus* pH.** *A,* WT, P0(+/−), P0(−/−); *B,* S63C(+/+), S63C(+/−), S63C(−/−). The nerves were incubated in solutions ranging in pH from 6.0 to 8.0 and at native ionic strength (154 mM). The different symbol sizes indicate the relative amount of myelin having that particular period. The *long arrows* pointing from the native-like period to the swollen period indicate the pH range at which the structural transition occurred. In WT, the shift was at pH 6.5–7.0, whereas in S63C(+/−), it occurred at pH 7.5–8.0. The difference suggests more alkaline pH is needed to stabilize the S63C(+/−) than the WT myelin. The *dashed lines* are the linear regressions for the P0(−/−) and S63C(−/−) data; and the standard errors for the periodicity were 7.1 Å for P0(−/−) and 2.6 Å for S63C(−/−).

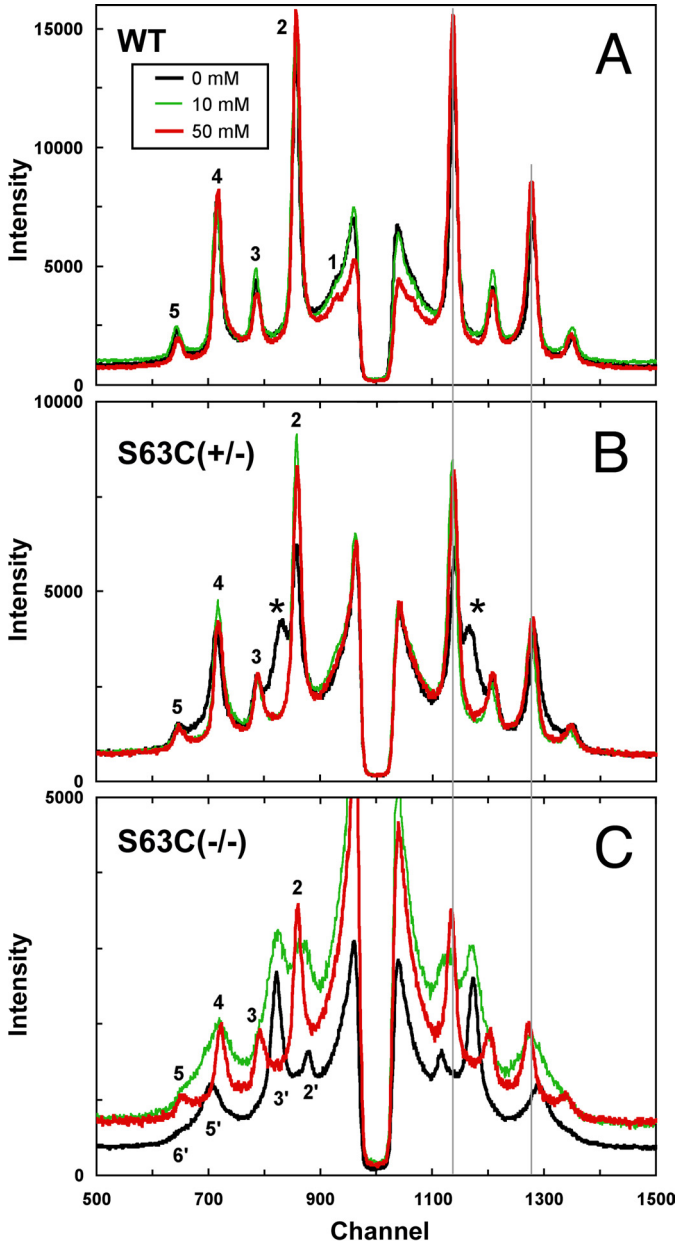

FIGURE 4. **Effect of reducing agent TCEP on swollen myelin in S63C peripheral nerve.** Diffraction patterns from WT (*A*), S63C(+/−) (*B*), and S63C(−/−) (*C*) sciatic nerves treated for 15–20 h with 0, 10, or 50 mM TCEP in 154 mM NaCl, 5 mM Tris base, pH 7.4. When S63C(+/−) was treated with 10 mM TCEP, the swollen array disappeared revealing only the native 176-Å period structure. When S63C(−/−) was treated with 10 mM TCEP, two arrays were seen (187 and ~222 Å), and after increasing the concentration of TCEP to 50 mM, only a single native period was observed. Bragg orders 2′, 3′, 5′, and 6′ index the swollen array, and 2–5 index the native array. The pair of *thin vertical lines* on the *right-hand side* that link the three panels indicate the positions of the 2nd and 4th order reflections for native period myelin.

of P0. Based on mRNA levels, the S63C(+/−) mice express 170% of normal P0 levels, and thus exhibit the overexpression phenotype of dose-dependent dysmyelination (10, 29). The S63C(−/−) expresses near normal P0 dosage (120% overexpression), but it lacks the Mpz^{WT}. The overexpression of P0 results in thinner myelin sheaths, which also could explain the hypomyelination observed in S63C(+/−). However, S63C(−/−) exhibits nearly normal P0 expression levels, indicating that the observed hypomyelination is independent of expression level and is caused by the mutation. The effect of the specific amino acid substitution can be additionally seen in the formation of two coexisting myelin arrays, swollen and native, with the swollen array of ~210 Å extremely stable in both S63C(+/−) and S63C(−/−). The swollen myelin is corroborated by EM in S63C(+/−) and S63C(−/−) sciatic nerves (10). Moreover, EM analysis of P0 overexpression (30–80% overexpression) reveals that the periodicity is apparently normal in the few thin myelin sheaths present (29). These points offer further validation that the structural changes in the sciatic nerves of S63C mice are due to the effects of the mutation rather than to the overexpression of P0.

S34C Most Likely Disrupted the Homophilic Binding Interface between Mutant and WT P0 Dimers—A dimeric, homophilic adhesion site involving amino acid residues His^{52} and $Arg^{45'}$ on the extracellular domains of opposing P0 molecules has been proposed (2). The cysteine (Cys^{34}) that substitutes for serine in the S63C mouse is in proximity to the pro-

TABLE 3

WT and P0 S34C sciatic nerves incubated with TCEP

The myelin structure was assessed by XRD in sciatic nerves incubated at physiological ionic strength (*i.e.* 154 mM NaCl, 5 mM Tris buffer, pH 7.4) with different concentrations of TCEP (see "Experimental Procedures").

TCEP	Dimension				Δ/*d*	Myelin	*M*/(*M*+*B*)
	d	cyt	lpg	*ext*			
mM		Å				%	
WT							
0	175.0	31	49	46	0.017		0.30
10	175.0	31	49	46	0.023		0.34
50	177.0	34	49	45	0.023		0.38
S63C(+/−)							
0	176.0	33	47	49	0.023	80	0.30
	218.7					20	
10	177.0	33	49	46	0.023		0.27
50	176.0	33	48	47	0.023		0.27
S63C(−/−)							
0	211.0	33	46	86	0.033		0.19
10	187.3					26	0.16
	222.3					74	
50	180.0	32	49	50	0.028		0.12

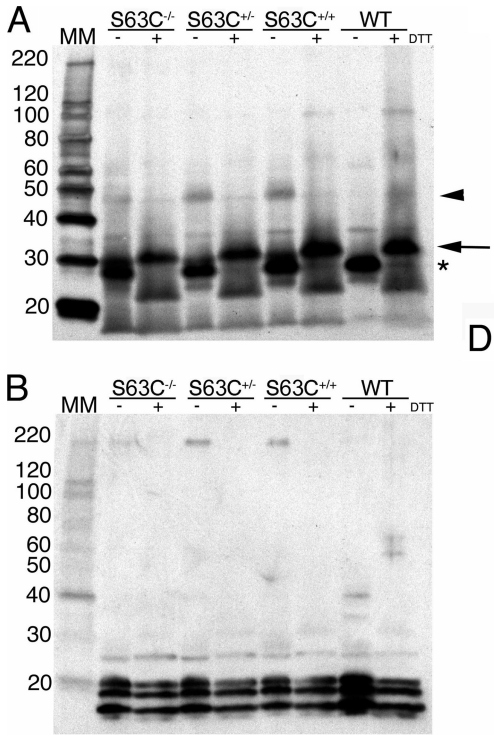

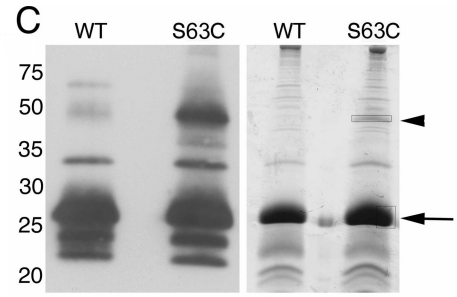

D

Peptides spanning residue Cys34 in the 27 KDa band

MH+	ppm	#Mod	Mod name	aa	sequence
997.47	-14	1	Carbamidomethyl	61-67	DICFTWR
1065.51	- 25	1	NEM	61-67	DICFTWR
1112.49	-6	1	Carbamidomethyl	60-67	DDICFTWR
1180.52	-9	1	NEM	60-67	DDICFTWR
1784.83	-5	1	Carbamidomethy	61-74	DICFTWRYQPEGGR
1899.84	2	1	Carbamidomethy	61-75	DICFTWRYQPEGGRD
1967.87	1	1	NEM	60-74	DDICFTWRYQPEGGR

Peptides spanning residue Cys34 in the 50 KDa band

MH+	ppm	#Mod	Mod name	aa	sequence
997.47	-14	1	Carbamidomethyl	61-67	DICFTWR
1112.49	-6	1	Carbamidomethyl	60-67	DDICFTWR
1784.83	-5	1	Carbamidomethyl	61-74	DICFTWRYQPEGGR
1899.84	2	1	Carbamidomethyl	61-75	DICFTWRYQPEGGRD

FIGURE 5. **S34C forms ectopic disulfide bonds.** *A,* myelin from sciatic nerves of adult mice was purified, separated using SDS-PAGE, under reducing and nonreducing conditions, and Western-blotted. P0 was detected using a rabbit polyclonal anti-P0 antibody (see "Experimental Procedures"). In the absence of DTT, P0 ran at ~27-kDa (*). In all the S63C transgenics, an additional band of around 50 kDa was detected (*arrowhead*). This band disappeared after treatment with DTT, which caused P0 to run at around 30 kDa (*arrow*). *B,* no modifications due to DTT were evident in MBP (detected using anti-MBP antibody), used as a loading control. *C,* Western blot and Coomassie gel of WT and S63C(+/+) purified myelin run under nonreducing conditions. In this Western blot, P0 was detected using a mouse monoclonal anti-P0 antibody. The two bands corresponding to the putative monomer and dimer (*arrow* and *arrowhead*, respectively) were excised for MALDI-TOF MS. Note that *Mpz*S63C is a transgene randomly inserted away from the *Mpz* locus. Therefore, S63C+/− is, for example, an abbreviation of *Mpz*S63C//*Mpz*+/− and contains the *Mpz*S63C transgene in addition to one wild type *Mpz* and one *Mpz* null allele. *D, tables* showing the peptides containing the Cys^{34} residue identified via MALDI-TOF MS in the 27- and 50-kDa bands. *MH+*, monoisotopic measured mass of the peptide; *#Mod*, number of modifications; *ppm*, part per million mass difference (measured mass-computed mass). Note that in the tables the amino acids are numbered according to the preprotein, including the 29-amino acid signal peptide (therefore, Cys^{34} is at position 63).

posed dimer interface and could destabilize the interaction between the histidine imidazole ring (His^{52}) and arginine guanidine group ($Arg^{45'}$) (2, 3) by formation of a *cis*-cysteine-histidine interaction due to p*K* shifts (Table 4). We propose that perturbation of the local electrostatic interaction could account for the pK_a shift. The proton dissociation constant (pK_a) of the residues in the crystallographic model of the ex-

TABLE 4

pK_a values of the His^{52} and Arg^{45} in monomer and dimer

Amino acid	Monomer	WT dimer	S34C(+/+) dimer
Cys^{34}			0.96
His^{52}	6.43	4.24	10.24
Arg^{45}	12.50	12.08	12.08

tracellular domain (rat extracellular domain, Protein Data Bank code 1NEU; Table 4) was determined using PROPKA (30). When the atomic coordinates of the P0wt dimer were used for the calculation, the pK_a of His^{52} was found to be pH 4.24, likely due to the local increase in [OH^-] concentration arising from the electrostatic influence of the Arg$^{45'}$ residue on the opposing P0 molecule. Swiss Viewer was used to construct the atomic structure of the dimeric P0 extracellular domain containing the point mutation S34C from the x-ray crystal structure of rat P0, and it subsequently was energy-minimized to make it stereochemically reasonable. When the pK_a values for the Cys^{34} mutant were estimated by PROPKA (Table 4) (30), the substitution resulted in a pK shift to pH 10.24 for His^{52} and to pH 0.96 for Cys^{34} (31–35). This would result in deprotonation of the cysteine thiol by the positively charged histidine, with formation of a *cis* cysteine-histidine interaction, which would be expected to weaken the His^{52}–Arg$^{45'}$ interaction, facilitating swelling. Thus, a positive-charged P0 dimer interface can account for swelling in S63C(+/−) myelin.

Novel Disulfide Accounted for Swollen Arrays in S63C(+/−) and S63C(−/−) Myelin—As the amino acid substituent is a cysteine residue and the P0 interactions are homophilic, we examined the possibility that formation of a disulfide bond might stabilize the swollen myelin. When S63C(+/−) and S63C(−/−) were treated with TCEP (thiol-free reducing agent), the swollen arrays disappeared (Fig. 4, *B* and *C*), whereas WT, under the same conditions, remained unaltered in period (Fig. 4*A*). The decrease in period was accounted for by a large reduction of the width in the extracellular apposition (Table 3). Modeling this disulfide bond between P0 extracellular domains from the crystal structure revealed that if a Cys^{34}–Cys$^{34'}$ disulfide forms, then the width of the extracellular apposition should measure ~70 Å (Fig. 6*B*), which is close to that observed for S63C(−/−) (Table 3), compared with the ~47 Å spacing found in the WT (Fig. 6*A*) (2, 36).

During PNS myelin development, the Schwann cell elaborates its plasma membrane, which initially loosely spirals around a single axon. During further development, the membrane forms a more regular spiral (37). EM thin sections indicate that at the initial stages of myelination, the extracellular apposition is widened with a regular gap at the same time that cytoplasm persists in the cytoplasmic space between membranes (see Figs. 6 and 7 and page 231 in Ref. 37). As myelination proceeds, the extracellular gap narrows, and the residual cytoplasm is lost, forming the major dense line and double intraperiod line at the cytoplasmic and extracellular apposition, respectively. In modeling the extracellular domain of P0, we hypothesized that the apposed molecules would align head-to-head during myelination, and subsequently slip by one another, overlapping to form dimers leading to the compaction and native periodicity of myelin (3). This head-to-head model is consistent with the developmental changes in the extracellular apposition as visualized using EM (described above). As the peripheral myelin compacts during development in the S63C mice, the location of the Cys^{34} residues on apposing membranes apparently allows formation of a disulfide bond. In the S63C(−/−), all dimeric interactions between

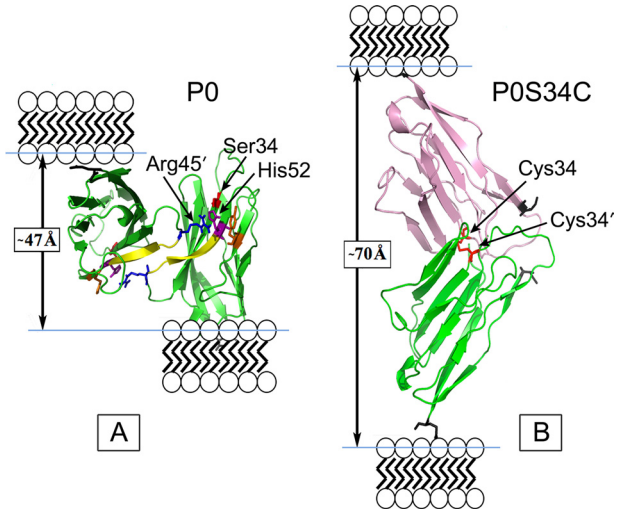

FIGURE 6. **Pymol representation of the WT (*A*) and modified (*B*) dimer interface of residues 45–52 of the P0S34C mutant extracellular domain.** The WT dimer shows one of the extracellular domains tilted back to reveal better the 2-fold interface. In the WT packing, the distance between the C termini (Glu^{119}, denoted by the *black skeletal model*) in the membrane stacking direction was measured to be ~47 Å (*arrow*). In the swollen myelin, the putative disulfide S34C-S′34C′ dimer gives a distance ~70 Å between the C termini (*arrow*) in the membrane stacking direction. Ionizable key residues influencing the electrostatic potential at the dimer interface, including Arg^{45}, His^{52}, and Tyr^{59}, are labeled. The N-terminal Ile^1 is indicated by the *gray skeletal model*. For the modeling, the two P0 molecules were translated and rotated using XtalView so that the Cys^{34} and Cys$^{34'}$ were correctly positioned to form a disulfide bond, and then the structure was energy-minimized using the GROMOS96 implementation of Swiss-PdbViewer.

the P0 tetrameric assemblies of opposing membranes are dictated by the disulfide bond, giving rise to the stable swollen period of ~210 Å observed by XRD. The widened period is due to the expansion of the extracellular space by ~70 Å, from the crystal structure (Fig. 6), and indicated by XRD analysis of unfixed sciatic nerve of S63C mice. In the P0 S63C(+/−) myelin, the disulfide bond apparently forms only in cases where two mutant proteins interact at the 2-fold dimeric interface. This would result in only a small amount of swollen myelin, as confirmed by XRD, which showed that ~20% of the myelin was swollen.

An overview of the diffraction data for the predominant myelin arrays in unfixed nerves from the genotypes examined here (supplemental Fig. 2) shows that there was no significant difference in periodicity among WT, S63C(+/+), and S63(+/−). These three did, however, differ significantly in period from S63C(−/−), P0(+/−), and P0(−/−). In fact, the consistently smaller period for S63C(+/−) compared with P0(+/−) indicates that the myelin having P0S34C is somewhat more adhesive than myelin with P0wt. At higher concentrations of the substituted protein (P0S34C), the *trans* disulfide bonds predominate, and the periodicity of S63C(−/−) myelin greatly exceeds that of P0(+/−).

In this study, we provide several strands of evidence in support of these *trans* disulfide bonds. TCEP is a thiol-free reducing agent that is more effective than both oxidized DTT or mercaptoethanol (17). XRD analysis demonstrated that incubation of sciatic nerves of S63C mice in TCEP/physiological saline at pH 7.4 led to reversion of the swollen arrays to native periodicity (~180 Å). Moreover, Western blot analysis of my-

elin revealed an ~50-kDa band under nonreducing conditions that was also abolished under reducing conditions. This band, identified using two different P0 antibodies, contained P0 as it was not detected in P0 null myelin analyzed in parallel by both Western blot and mass spectrometric analyses. Finally, alkylation followed by reduction and mass spectrometry identified only Cys^{34}-containing peptides in the 50-kDa band, and then only in the oxidized state, although we identified both Ser^{34} and Cys^{34} peptides in both the reduced and oxidized state in the 27-kDa band. The sum of these data strongly supports that some P0S34C are bound covalently by *trans* disulfide bonds, which likely account for the swollen myelin.

The possibility that Cys^{34} is also covalently bound with the normal endogenous Cys^{21} or Cys^{98} cannot be eliminated because we have not directly identified Cys^{34}=Cys^{34} dimer-containing peptides. However, we identified Cys^{21} in the oxidized state (and not Cys^{98}) only in the 27-kDa band and not in the 50-kDa. Finally, such Cys^{34}=Cys^{21} or Cys^{34}=Cys^{98} dimers would require a significant level of unfolding to expose Cys^{21} or Cys^{98}. Unfolding of other P0 mutants, such as P0S34del, causes retention of the mutant protein in the endoplasmic reticulum and blocks arrival to myelin (10, 38). Thus, these P0-P0 covalent dimers are unlikely to be found in internodal myelin of S63C mice. (An additional cysteine at position 153 is intracellular and is therefore inaccessible to Cys^{21} or Cys^{98} in the extracellular domain of P0.)

Genotype/Phenotype Considerations—We envision two mechanisms by which P0=P0 dimer formation that is *trans* head-to-head and covalent could cause the mixed hypomyelinating/demyelinating neuropathy documented in S63C nerves (10). First, formation of *trans* covalent dimers during myelination would likely arrest mesaxonal wrapping, such as has been suggested for premature noncovalent adhesion in developing nerves in P0-overexpressing transgenic mice (29, 39). This provides further evidence for the idea that P0 interactions in *trans* must be carefully regulated during wrapping.

Second, in mature (albeit thin) myelin, the presence of P0wt in the hemizygous transgenic nerves would introduce heterogeneous homophilic (sometimes covalent) interactions, leading to inconsistent packing and the instability observed by XRD analysis. This local instability could alter the dynamic inter-membrane interactions of myelin, which at a more macroscopic scale could result in damage to some internodes and myelin destruction. This model is supported by the finding of onion bulbs in S63C nerves, suggesting demyelination followed by inefficient remyelination (as in mechanism 1 above).

Altered myelin structure ultimately leads to phenotypic neuropathies, given that myelin packing and nerve conduction are intimately connected. For example, studies in the Trembler mouse mutant, which has a defect in the myelin *PMP-22* gene (40, 41), show a reduction of axonal diameter (42), altered slow axonal transport, altered regeneration of the axon (43), decrease in neurofilament (NF) phosphorylation, and an increase in NF density (44). One striking aspect of the changes in NF phosphorylation is the concomitant decrease in axon diameter in areas of the axon where there is demyelination (44). The other segments of the same axon may be unaffected, resulting in the Schwann cell affecting local axonal morphology, in turn altering neuronal function of the entire axon. Axonal diameter increases the speed of action potential conduction, and the changes in NF density and NF phosphorylation effectively alter the electrophysiology of the nerves (44). Alterations such as these have also been documented in diabetic neuropathies (45, 46) and in hereditary neuropathies including Charcot-Marie-Tooth and DSS (47, 48). Also, in a nerve biopsy from a CMT1A patient, a reduction in axonal caliber and evidence of NF dephosphorylation were observed (48). These changes can lead to axonal degeneration, particularly in the distal regions, resulting in irreversible clinical consequences, such as muscle atrophy and sensory dysfunction (49).

REFERENCES

1. Kirschner, D. A., Wrabetz, L., and Feltri, M. L. (2004) in *Myelin Biology and Disorders* (Lazzarini, R. A., Griffin, J. W., Lassmann, H., Nave, K. A., Miller, R. H., and Trapp, B. D., eds) pp. 523–545, Elsevier/Academic Press, Amsterdam
2. Shapiro, L., Doyle, J. P., Hensley, P., Colman, D. R., and Hendrickson, W. A. (1996) *Neuron* **17,** 435–449
3. Wells, C. A., Saavedra, R. A., Inouye, H., and Kirschner, D. A. (1993) *J. Neurochem.* **61,** 1987–1995
4. Kirschner, D. A., and Ganser, A. L. (1980) *Nature* **283,** 207–210
5. Giese, K. P., Martini, R., Lemke, G., Soriano, P., and Schachner, M. (1992) *Cell* **71,** 565–576
6. Martini, R., Mohajeri, M. H., Kasper, S., Giese, K. P., and Schachner, M. (1995) *J. Neurosci.* **15,** 4488–4495
7. Hayasaka, K., Himoro, M., Sawaishi, Y., Nanao, K., Takahashi, T., Takada, G., Nicholson, G. A., Ouvrier, R. A., and Tachi, N. (1993) *Nat. Genet.* **5,** 266–268
8. Shy, M. E., Jáni, A., Krajewski, K., Grandis, M., Lewis, R. A., Li, J., Shy, R. R., Balsamo, J., Lilien, J., Garbern, J. Y., and Kamholz, J. (2004) *Brain* **127,** 371–384
9. Shy, M. E., Garbern, J. Y., and Kamholz, J. (2002) *Lancet Neurol.* **1,** 110–118
10. Wrabetz, L., D'Antonio, M., Pennuto, M., Dati, G., Tinelli, E., Fratta, P., Previtali, S., Imperiale, D., Zielasek, J., Toyka, K., Avila, R. L., Kirschner, D. A., Messing, A., Feltri, M. L., and Quattrini, A. (2006) *J. Neurosci.* **26,** 2358–2368
11. Kirschner, D. A., and Saavedra, R. A. (1994) *J. Neurosci. Res.* **39,** 63–69
12. Kirschner, D. A., Szumowski, K., Gabreëls-Festen, A. A., Hoogendijk, J. E., and Bolhuis, P. A. (1996) *J. Neurosci. Res.* **46,** 502–508
13. Warner, L. E., Hilz, M. J., Appel, S. H., Killian, J. M., Kolodry, E. H., Karpati, G., Carpenter, S., Watters, G. V., Wheeler, C., Witt, D., Bodell, A., Nelis, E., Van Broeckhoven, C., and Lupski, J. R. (1996) *Neuron* **17,** 451–460
14. Kirschner, D. A., and Blaurock, A. E. (1992) in *Myelin: Biology and Chemistry* (Martenson, R. E., ed) pp. 3–78, CRC Press, Inc., Boca Raton, FL
15. Avila, R. L., Inouye, H., Baek, R. C., Yin, X., Trapp, B. D., Feltri, M. L., Wrabetz, L., and Kirschner, D. A. (2005) *J. Neuropathol. Exp. Neurol.* **64,** 976–990
16. Inouye, H., and Kirschner, D. A. (1988) *Biophys. J.* **53,** 235–245
17. Han, J. C., and Han, G. Y. (1994) *Anal. Biochem.* **220,** 5–10
18. Levison, M. E., Josephson, A. S., and Kirschenbaum, D. M. (1969) *Experientia* **25,** 126–127
19. Agrawal, D., Hawk, R., Avila, R. L., Inouye, H., and Kirschner, D. A. (2009) *J. Struct. Biol.* **168,** 521–526
20. Yin, X., Baek, R. C., Kirschner, D. A., Peterson, A., Fujii, Y., Nave, K. A., Macklin, W. B., and Trapp, B. D. (2006) *J. Cell Biol.* **172,** 469–478
21. Alexander, L. E. (1979) *X-ray Diffraction Methods in Polymer Science*, Krieger, Huntington, NY
22. Inouye, H., Karthigasan, J., and Kirschner, D. A. (1989) *Biophys. J.* **56,** 129–137
23. Norton, W. T., and Poduslo, S. E. (1973) *J. Neurochem.* **21,** 749–757

24. Shevchenko, A., Wilm, M., Vorm, O., and Mann, M. (1996) *Anal. Chem.* **68,** 850–858
25. Kirschner, D. A., and Hollingshead, C. J. (1980) *J. Ultrastruct. Res.* **73,** 211–232
26. Blaurock, A. E., Genter St Clair, M. B., and Graham, D. G. (1991) *Neuropathol. Appl. Neurobiol.* **17,** 309–321
27. Flores, A. I., Narayanan, S. P., Morse, E. N., Shick, H. E., Yin, X., Kidd, G., Avila, R. L., Kirschner, D. A., and Macklin, W. B. (2008) *J. Neurosci.* **28,** 7174–7183
28. Ouvrier, R. A., McLeod, J. G., and Conchin, T. E. (1987) *Brain* **110,** 121–148
29. Wrabetz, L., Feltri, M. L., Quattrini, A., Imperiale, D., Previtali, S., D'Antonio, M., Martini, R., Yin, X., Trapp, B. D., Zhou, L., Chiu, S. Y., and Messing, A. (2000) *J. Cell Biol.* **148,** 1021–1034
30. Li, H., Robertson, A. D., and Jensen, J. H. (2005) *Proteins* **61,** 704–721
31. Jez, J. M., and Noel, J. P. (2000) *J. Biol. Chem.* **275,** 39640–39646
32. Lewis, S. D., Johnson, F. A., and Shafer, J. A. (1976) *Biochemistry* **15,** 5009–5017
33. Lewis, S. D., Johnson, F. A., and Shafer, J. A. (1981) *Biochemistry* **20,** 48–51
34. Pinitglang, S., Watts, A. B., Patel, M., Reid, J. D., Noble, M. A., Gul, S., Bokth, A., Naeem, A., Patel, H., Thomas, E. W., Sreedharan, S. K., Verma, C., and Brocklehurst, K. (1997) *Biochemistry* **36,** 9968–9982
35. Whitaker, J. R., and Bender, M. L. (1965) *J. Am. Chem. Soc.* **87,** 2728–2737
36. Kirschner, D. A., Inouye, H., Ganser, A. L., and Mann, V. (1989) *J. Neurochem.* **53,** 1599–1609
37. Peters, A., Palay, S. L., and Webster, H. D. (1991) *The Fine Structure of the Nervous System: Neurons and Their Supporting Cells*, 3rd Ed., Oxford University Press, New York
38. Pennuto, M., Tinelli, E., Malaguti, M., Del Carro, U., D'Antonio, M., Ron, D., Quattrini, A., Feltri, M. L., and Wrabetz, L. (2008) *Neuron* **57,** 393–405
39. Yin, X., Kidd, G. J., Wrabetz, L., Feltri, M. L., Messing, A., and Trapp, B. D. (2000) *J. Cell Biol.* **148,** 1009–1020
40. Suter, U., Moskow, J. J., Welcher, A. A., Snipes, G. J., Kosaras, B., Sidman, R. L., Buchberg, A. M., and Shooter, E. M. (1992) *Proc. Natl. Acad. Sci. U.S.A.* **89,** 4382–4386
41. Suter, U., Welcher, A. A., Ozcelik, T., Snipes, G. J., Kosaras, B., Francke, U., Billings-Gagliardi, S., Sidman, R. L., and Shooter, E. M. (1992) *Nature* **356,** 241–244
42. Aguayo, A. J., Attiwell, M., Trecarten, J., Perkins, S., and Bray, G. M. (1977) *Nature* **265,** 73–75
43. de Waegh, S., and Brady, S. T. (1990) *J. Neurosci.* **10,** 1855–1865
44. de Waegh, S. M., Lee, V. M., and Brady, S. T. (1992) *Cell* **68,** 451–463
45. Medori, R., Autilio-Gambetti, L., Jenich, H., and Gambetti, P. (1988) *Neurology* **38,** 597–601
46. Medori, R., Jenich, H., Autilio-Gambetti, L., and Gambetti, P. (1988) *J. Neurosci.* **8,** 1814–1821
47. Martini, R. (2001) *Muscle Nerve* **24,** 456–466
48. Watson, D. F., Nachtman, F. N., Kuncl, R. W., and Griffin, J. W. (1994) *Neurology* **44,** 2383–2387
49. Bjartmar, C., Yin, X., and Trapp, B. D. (1999) *J. Neurocytol.* **28,** 383–395
50. Kirschner, D. A., and Caspar, D. L. (1975) *Proc. Natl. Acad. Sci. U.S.A.* **72,** 3513–3517